Japanese Journal of Applied Physics
Vol. 46, No. 38, 2007, pp. L942–L944

Atmospheric Pressure Remote Plasma Ashing of Photoresist Using Pin-To-Plate Dielectric Barrier Discharge

Jaebeom PARK, Sejin KYUNG, and Geunyoung YEOM*

Department of Advanced Materials Science and Engineering, Sungkyunkwan University, Suwon, Kyunggi-do 440-746, South Korea

(Received June 14, 2007; accepted August 16, 2007; published online September 28, 2007)

Plasma ashing of photoresist (PR) was investigated with $N_2/O_2/SF_6$ gas mixtures using remote-type atmospheric pressure plasma generated by a pin-to-plate type dielectric barrier discharge. When a certain amount of O_2 and SF_6 were added together to N_2, higher PR ashing achieved at N_2 (70 slm)/O_2 (200 sccm)/SF_6 (3 slm). [DOI: 10.1143/JJAP.46.L942]

KEYWORDS: DBD, remote-type atmospheric pressure plasma, PR ashing, $N_2/O_2/SF_6$ gas mixture, glow discharge

These days, many researchers are developing glow discharges generated at atmospheric pressure for thin film and surface processing. Various types of atmospheric pressure cold plasmas were reported from different groups, and are claimed to have advantages of low running cost, low gas temperature, and wide applicability to surface modification, etching, thin film deposition, etc.[1–3] For the above processing, numerous atmospheric pressure plasma sources, for example, radio frequency plasma torch, dielectric barrier discharge (DBD), microwave discharge, pulsed corona plasma, etc.[4–6] have been studied. Among the various atmospheric pressure plasmas discharge sources, the DBD which is consisted of two parallel electrodes covered by dielectric plates has been studied most widely due to the easier generation of stable glow discharges.

Direct plasma-type DBD is currently applied to the modification or cleaning of the surface of metals, polymers, glasses, printed circuit boards, or plasma display by locating the materials to be treated between the two dielectric covered electrodes. But, arcing is frequently observed during the operation of the DBD and the substrate is more likely to be damaged during the processing. Therefore, the use of the DBD to other application areas such as plasma ashing, etching, and thin film deposition is limited due to the damage on the surface during the processing in addition to a problem of low processing rate due to low plasma density of the conventional DBD source. Also, thermal damage can occur due to the direct contact of the plasma on the substrate. These disadvantages can be overcome by using a remote plasma-type. Because remote plasma does not contact the substrate directly, the substrate can avoid from any kind of radiation damage from the plasma. And added benefit is that one may also have more control over radical flux.[7,8)]

In this study, plasma ashing of photoresist (PR) has been studied using a remote-type DBD. Especially, to increase the plasma density of the DBD, a modified DBD known as "pin-to-plate DBD" which has a multi-pin electrode instead of a blank electrode as the power electrode has been used and the effect of gas combination of $N_2/O_2/SF_6$ on the PR ashing characteristics and the discharge characteristics was investigated.

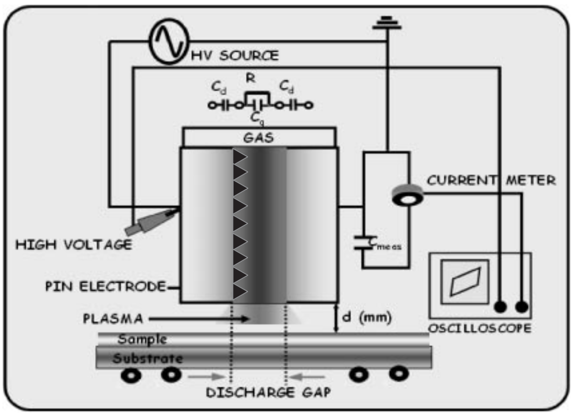

Fig. 1. Schematic diagram of the remote-type atmospheric pressure discharge system (pin-to-plate DBD) used in the experiment.

Figure 1 shows the schematic diagram of the remote plasma-type DBD system used in the experiment. The discharge source was composed of a multi-pin power electrode and a blank ground electrode located vertically above the substrate. The electrodes were made of aluminum and the size of the electrode was $100 \times 170\,\text{mm}^2$. The power electrode was machined to have multi-pins as shown in Fig. 1 and the both of the electrodes were coated with 300-µm-thick alumina. In the figure, C_d (C_{d1}: for power electrode, C_{d2}: for ground electrode) is the capacitance by the dielectrics on the both electrodes, C_g is the capacitance of air gap between the electrodes during the plasma-off period, and R is the resistance of the plasma between the electrodes during the plasma-on period.

The power electrode was connected to an AC power supply having the maximum frequency of 30 kHz and the maximum power of 4 kW. The input voltage to the power electrode was varied from 6.5 to 8 kV (rms voltage) in our study, and which ensured stable and uniform plasmas while the AC frequency was fixed at 30 kHz and the processing time was maintained at 30 s. N_2 gas was used as a feeding gas while SF_6 and O_2 were used for ashing gas. The soda lime glass covered with a PR was used as the substrate.

The rms voltage was measured with a high-voltage probe (Tektronix P6015A), and the discharge current was measured with a current meter (PEARSON™ Electonix 6600), and these electrical data were recorded on the oscilloscope (Tektronix TDS 340A) simultaneously to calculate the consumed power and the Q–V Lissajou curve. The PR ashing rate was estimated by measuring the ashing depth using a step profilometer (TENCOR alpha-step 500). Optical emission intensities of the species emitted from the plasma were measured using optical emission spectroscopy (OES; PCM 420 SC-Technology) in order to detect radicals or

---

*Corresponding author. E-mail address: gyyeom@skku.edu

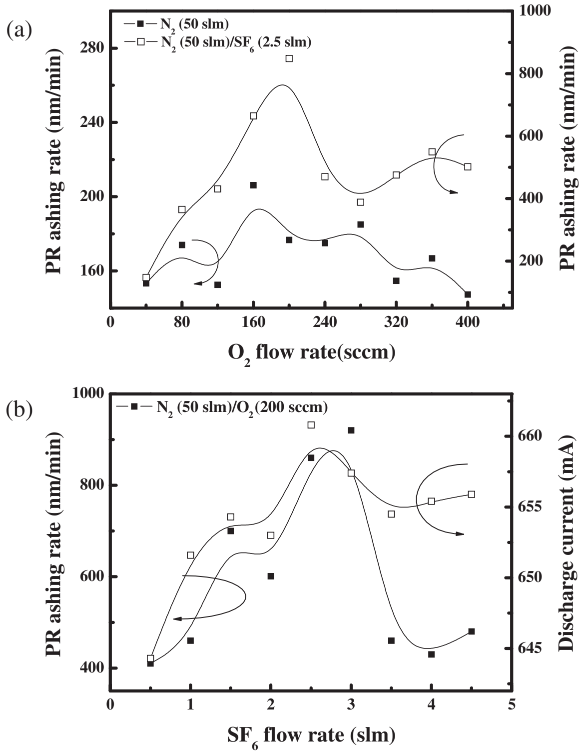

Fig. 2. (a) Effect of various gas combination such as N_2 (50 slm)/O_2 (0–400 sccm), N_2 (50 slm)/O_2 (0–400 sccm)/SF_6 (2.5 slm) on the PR ashing rate. (b) PR ashing rate and discharge current measured as a function of the SF_6 flow rate at N_2(50 slm)/O_2(200 sccm).

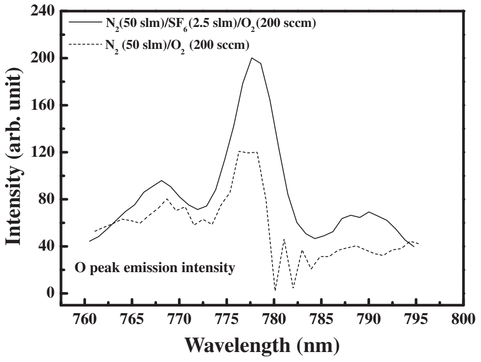

Fig. 3. Optical emission intensities of O peak measured for the discharges of N_2 (50 slm)/O_2 (200 sccm) and N_2 (50 slm)/O_2 (200 sccm)/SF_6 (2.5 slm).

activated species and to characterize the plasma.

Figure 2(a) shows the PR ashing rate measured as a function of O_2 for N_2 (50 slm)/O_2 (0–400 sccm) and N_2 (50 slm)/SF_6 (2.5 slm)/O_2 (0–400 sccm) for the remote plasma-type DBD. The input rms voltage to the power electrode was maintained at 8 kV. As shown in the figure, the increase of O_2 flow rate increased the PR ashing rate until 160 sccm of O_2 was added to N_2 (50 slm) or 200 sccm of O_2 was added to N_2 (50 slm)/SF_6 (2.5 slm), and the further addition of O_2 decreased the PR ashing rate. Also, the use of SF_6 in addition to O_2 increased the PR ashing rate further. The PR ashing rate in N_2 (50 slm)/O_2 (160 sccm) was about 206 nm/min while the PR ashing rate in N_2 (50 slm)/O_2 (200 sccm)/SF_6 (2.5 slm) was about 848 nm/min, therefore, about 4 times of PR ashing rate could be obtained by the addition of SF_6 (2.5 slm) in N_2/O_2. Figure 2(b) shows the effect of SF_6 flow rate added to N_2 (50 slm)/O_2 (200 sccm) on the PR ashing rate and the discharge current to the power electrode maintained at 8 kV of rms voltage. As shown in the figure, the addition of SF_6 also increased the PR ashing rate until 3 slm of SF_6 was added to N_2 (50 slm)/O_2 (200 sccm), however, the further increase of SF_6 flow rate decreased the PR ashing rate significantly. The discharge current measured at a fixed AC voltage showed the similar trend as the PR ashing rate, therefore, the highest discharge current was obtained 3 slm of SF_6. The maximum PR ashing rate of about 920 nm/min was obtained at N_2 (50 slm)/O_2 (200 sccm)/SF_6 (3 slm).

The increase of PR ashing rate with the addition of O_2 up to 160 and 200 sccm to N_2 (50 slm) and N_2 (50 slm)/SF_6 (2.5 slm), respectively, is believed to be related to the increase of dissociated O by the increase of O_2 addition to the gas composition. The increase of PR ashing rate with the addition of SF_6 to N_2 (50 slm)/O_2 (200 sccm) is also believed to be related to the increase of O_2 in addition to the increase of F in the plasma. The variation of O atomic density and F atomic density can be estimated by OES.[9] Figure 3 shows the O atomic emission intensities for N_2 (50 slm)/O_2 (200 sccm) and N_2 (50 slm)/O_2 (200 scccm)/SF_6 (2.5 slm). As shown in Fig. 3, the addition of SF_6 to N_2 (50 slm)/O_2 (200 sccm) increased the O emission intensity in addition to the F emission intensity possibly indicating the increase of O density by SF_6 due to a penning ionization/dissociation which causes the ionization/dissociation of O_2 further by the collision of metastable F with O_2 as studied by Massinesa *et al.*[10] However, the decrease of PR ashing rate with the addition of O_2 higher than 160 and 200 sccm to N_2 (50 slm) and N_2 (50 slm)/SF_6 (2.5 slm), respectively, and with the addition of SF_6 higher than 3 slm to N_2 (50 slm)/O_2 (200 sccm) is believed to related to the decrease of O and F atomic density by the change of the plasma from a glow discharge to an unstable filamentary discharge. The addition of O_2 and SF_6 to N_2 (50 slm) higher than a certain amount decreases electron density in the plasma by forming electronegative ions due to the high electronegativity of O and F and tends to form a filamentary discharge. The change of a glow discharge to a filamentary discharge could be observed by the decease of the optical emission peak intensity or by visual observation.

To understand the effect of SF_6 addition less than 3 slm to N_2 (50 slm)/O_2 (200 sccm) further, the *Q*–*V* Lissajou curves showing the electrical characteristics of the plasma were investigated. Figure 4(a) shows the parameters that can be obtained from the curve.[11] The actual power applied to the system can be obtained from the parallelogram-type area enclosed by the *Q*–*V* Lissajou curve shown in the figure. Also, from the slopes (Q/V) of the curve, the capacitances of the discharge system during the power-on and power-off period can be calculated. In addition, the point that the upper part of the *Q*–*V* Lissajou curve crosses the voltage axis is the discharge breakdown voltage. Figure 4(b) shows the *Q*–*V* Lissajou curves obtained for the plasmas with N_2 (50 slm)/O_2 (200 sccm) and N_2 (50 slm)/O_2 (200 sccm)/SF_6 (2.5 slm) at the 6 kV of input voltage. As shown in the figure, the plasma turn-on voltage for N_2 (50 slm)/O_2 (200 sccm) was 3.16 kV while that for N_2 (50 slm)/O_2 (200 sccm)/SF_6

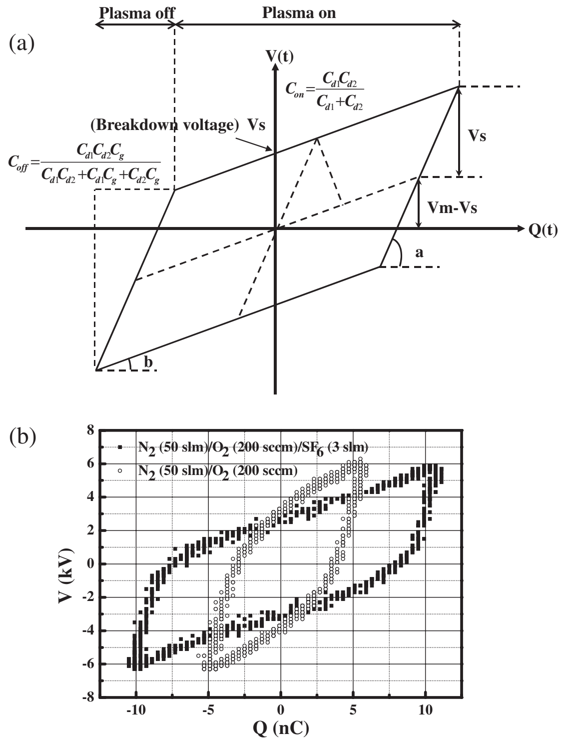

Fig. 4. (a) Typical Q–V Lossajou curve (Q–V oscillographic diagram) and the information from the curve. (b) Q–V Lissajou curves measured for the discharges of N_2 (50 slm)/O_2 (200 sccm) and N_2 (50 slm)/O_2 (200 sccm)/SF_6 (2.5 slm).

(2.5 slm) was 2.7 kV, therefore, a lower turn-on voltage was obtained by adding 2.5 slm of SF_6. Especially, at a given discharge voltage of 6 kV, the consumed power for N_2 (50 slm)/O_2 (200 sccm)/SF_6 (2.5 slm) was 2330 W while that for N_2 (50 slm)/O_2 (200 sccm) was 1119 W, therefore, the addition of 2.5 slm of SF_6 increased the power consumption in the plasma by ionizing and dissociation the gas mixture further possibly through the penning ionization and dissociation as described above.

For the optimization of the PR ashing process, N_2 in the gas mixture composed of N_2/O_2 (200 sccm)/SF_6 (3 slm) was varied and the effect of N_2 flow rate on the PR ashing rate and the optical emission intensities of O and F were investigated and the results are shown in Fig. 5. The input voltage was 8 kV. As shown in Fig. 5, the increase of N_2 flow rate increased the PR ashing rate until 70 slm is reached. The optical emission intensities of O and F were also increased with the increase of N_2 flow rate up to 70 slm. In the remote plasma sources, active species are transported from the plasma source to the substrate. In this experiment, the optical emission intensities are measured at the location between the source and the substrate. Therefore, the increase of optical emission intensities from O and F atoms is related to the increased transport of the species to the substrate before recombination. The saturation of the optical emission intensities measured for N_2 flow rate higher than 70 slm is believed to be from the limitation on the amount of the active species generated at the source area. The maximum PR ashing rate obtained in this study was about 1850 nm/min at the gas mixture of N_2 (70 slm)/O_2 (200 sccm)/SF_6 (3 slm) and with the input voltage of 8 kV at 30 kHz.

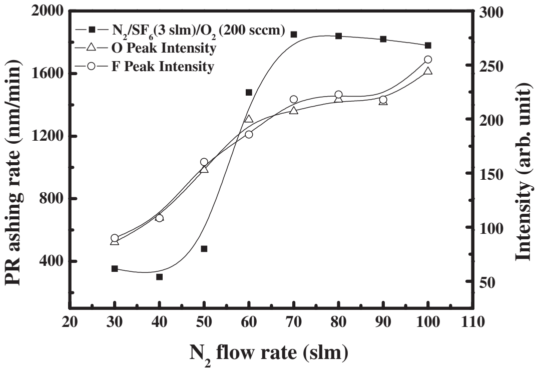

Fig. 5. The PR ashing rate and O and F optical emission intensities as a function of N_2 flow rate (30–100 slm) with O_2 (200 sccm)/SF_6 (3 slm).

In this study, atmospheric pressure remote plasmas were generated by using a modified DBD called "pin-to-plate DBD" and the effect of gas combinations of $N_2/O_2/SF_6$ on the effect of PR ashing rate and its plasma characteristics were investigated. The addition of oxygen (<200 sccm) to N_2 (50 slm) and N_2 (50 slm)/SF_6 (2.5 slm) and the addition of SF_6 (<3 slm) to N_2 (50 slm)/O_2 (200 sccm) increased the PR ashing rate due to the increase of active dissociated species in the plasma. Especially, compared to the gas mixture of N_2 (50 slm)/O_2 (200 sccm), N_2 (50 slm)/O_2 (200 sccm)/SF_6 (2.5 slm) showed the higher PR ashing rate due to the enhanced dissociation of O_2 in addition to the active F atoms from SF_6. The addition of 2.5 slm of SF_6 to N_2 (50 slm)/O_2 (200 sccm) decreased the plasma turn-on voltage, increased the discharge current and consumed power, therefore, higher plasma density could be obtained by the addition of 2.5 slm of SF_6 possibly through the penning ionization. However, the further increase of O_2 and SF_6 decreased the PR ashing rate due to the decrease in the active dissociated species by the transition of the plasma from a glow discharge to a filamentary discharge. By optimizing $N_2/O_2/SF_6$ gas mixtures, the highest PR ashing rate of 1850 nm/min could be achieved at N_2 (70 slm)/O_2 (200 sccm)/SF_6 (3 slm).

This work was supported by the National Program for Tera-level Nanodevices of the Korea Ministry of Science and Technology as one of the 21st Century Frontier Programs.

1) S. Okazaki, M. Kogoma, M. Uehara, and Y. Kimura: J. Phys. D **26** (1993) 889.
2) T. Yokoyama, M. Kogoma, S. Kanazawa, T. Moriwaki, and S. Okazaki: J. Phys. D **23** (1990) 374.
3) T. Yokoyama, M. Kogoma, T. Moriwaki, and S. Okazaki: J. Phys. D **23** (1990) 1125.
4) C. Tendero, C. Tixier, P. Tristant, J. Desmaison, and P. Leprince: Spectrochim. Acta, Part B **61** (2006) 2.
5) E. E. Kunhardt: IEEE Trans. Plasma Sci. **28** (2000) 189.
6) A. Schutze, J. Y. Jeong, S. E. Babayan, J. Y. Park, G. S. Selwyn, and R. F. Hicks: IEEE Trans. Plasma Sci. **26** (1998) 1685.
7) G. R. Nowling, S. E. Babayan, V. Jankovic, and R. F. Hicks: Plasma Sources Sci. Technol. **11** (2002) 97.
8) M. J. Kushner: J. Appl. Phys. **71** (1992) 4173.
9) R. Payling and P. Larkins: *Optical Emission Lines of the Elements* (John Wiely & Sons, Chichester, 2004).
10) F. Massinesa, P. Ségurb, N. Gherardi, C. Khamphan, and A. Ricard: Surf. Coat. Technol. **174–175** (2003) 8.
11) Y.-H. Lee, S.-J. Kyung, C.-H. Jeong, and G.-Y. Yeom: Jpn. J. Appl. Phys. **44** (2005) L78.